International Journal of Ocean System Engineering 3(4) (2013) 164-168
http://dx.doi.org/10.5574/IJOSE.2013.3.4.164

Design Load Analysis of Current Power Rotor and Tower Interaction

Chul H. Jo[1], Kang-Hee Lee[1], Su-Jin Hwang[1] and Jun-Ho Lee[1*]

[1]*Department of Naval Architecture and Ocean Engineering, Inha University*

(Manuscript Received September 8 2013; Revised October 12, 2013; Accepted November 8, 2013)

Abstract

Tidal-current power is now recognized as a clean power resource. The turbine blade is the fundamental component of a tidal current power turbine. The kinetic energy available within a tidal current can be converted into rotational power by turbine blades. While in service, turbine blades are generally subjected to cyclic fatigue loading due to their rotation and the rotor–tower interaction. Predicting the fatigue life under a hydrodynamic fatigue load is very important to prevent blade failure while in service. To predict the fatigue life, hydrodynamic load data should be acquired. In this study, the vibration characteristics were analyzed based on three-dimensional unsteady simulations to obtain the cyclic fatigue load. Our results can be applied to the fatigue design of horizontal-axis tidal turbines.

Keywords: Rotor–tower interaction, Computational fluid dynamics (CFD), Vibration, Horizontal-axis turbine (HAT), Renewable energy

1. Introduction

A tidal current power (TCP) system uses tidal current by converting kinetic energy into rotational energy to generate electricity. In general, there are two types of TCP systems: horizontal-axis turbines (HATs) and vertical-axis turbines (VATs). The turbine converts tidal current energy into rotational energy.

Recently, TCP system capacities have become greater than 1 MW per TCP turbine. Turbines are being designed with diameters of 18 to 20 m. Interest in the stability evaluation of TCP structures is increasing as their structural loads increase. Whenever turbine blades pass the tower, vibration and load fluctuations are generated because of pressure and vorticity changes between the blades and the tower. This is called the "rotor–tower interaction." TCP stability research has been performed using the fluid–structure interaction (FSI) method [1], and research on the oscillatory motion of a TCP turbine [2] has been conducted. However, few studies of the rotor–tower interaction have been performed. Many studies have been performed in the wind-power field, such as analyses of the rotor–tower interaction using a BEMT model [3] and analyses of the unsteady turbine–tower interaction [4]. In addition, a simulation of the TCP rotor–foundation interaction was performed in Germany [5]. The impact of the rotor–tower interaction on the power output of a fixed-speed wind farm was observed in the UK [6].

In this study, load signals and pressure fluctuations that could cause a fatigue problem were analyzed using unsteady CFD calculations.

2. CFD Analysis

In this study, a numerical analysis based on three-dimensional (3-D) Reynolds-averaged Navier–

*Corresponding author. Tel.: +82-32-860-7342, Fax.: +82-32-864-5850
E-mail address: ljunh330@inha.edu

Fig. 1. 3-D model of TCP

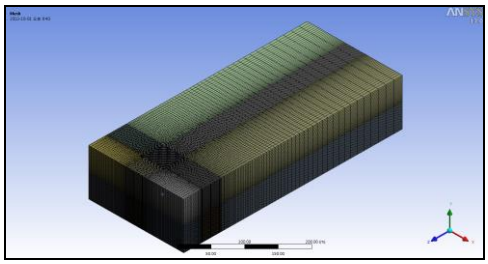
Fig. 2. Grid system

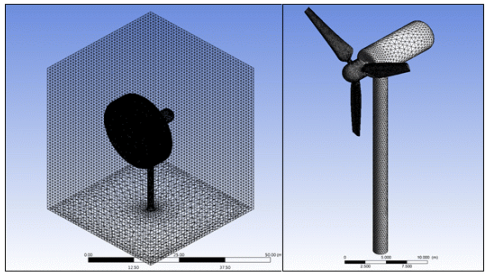
Fig. 3. Grid system of inner zone

Stokes (RANS) equations was used for the flow analysis of turbo-machinery, which greatly reduced the time and cost associated with experimental testing. A computational fluid dynamics (CFD) analysis was conducted to estimate the rotor–tower interaction. The ANSYS CFX commercial CFD code (version 13.0) was used for the simulations.

2.1 Modeling

The TCP rotor and tower had diameters of 20 m and 1.8 m, respectively, and the distance between the blades and tower was 3 m. An S814 rotor airfoil was selected, which has been applied to the SeaGen TCP system of MCT's SeaGen. The rotor and tower geometry information is listed in Table 1. A 3-D solid model of the rotor and tower are shown in Fig. 1.

2.2 Grid System

Grid generation was carefully conducted for smooth convergence and reliable results. The thickness of the near-wall grid layers and the aspect ratio of the mesh were considered according to the application of the turbulence model. The key area around the rotating blades and tower was considered to be the key area of interest for an accurate estimation of the pressure and force. Thus, a dense tetra-prism mesh was generated in the inner zone, which has a rotating domain and tower. We concentrated cells around the rotor and tower. A structural mesh was generated in the outer zone. The grid systems of the inner zone and outer zone are shown in Figs. 2 and 3, respectively. The mesh information is described in Table 2.

2.3 Boundary Condition

The rotor, tower, and bottom were defined as non-slip walls. In the rotating domain, an angular velocity was prescribed for TSR 5, which has a maximum power coefficient. A normal design velocity of 3.0 m/s was applied to the inlet. The static pressure was set to 1.0 atm at the outlet. The surfaces between the two domains were interfaced using the general grid interface (GGI) method. The shear stress transport (SST) turbulence model was used as a turbulence closure. In the SST model, a k-ω model was used at the near-wall, and a k-ε model was used beyond the wall region. The distances from the rotor were 5D to the inlet, 5D to the side , and 20D to the outlet. The total analysis time was 12 s, and the time step was set at 0.015 s. In order to increase the accuracy of the unsteady analysis, a second-order backward Euler scheme was selected. Table 3 lists the defined boundary conditions.

Table 1. Geometry of rotor and tower

	Rotor	Tower
Diameter (m)	20	1.8
Airfoil	S814	-
Number of blades	3	-
Height (m) (from bottom to hub)	-	30

Table 2. Mesh information

Inner zone	Nodes	1,051,886
	Elements	5,845,642
Outer zone	Nodes	846,038
	Elements	840,400

2.4 Computational Cost

The computations were performed on a PC equipped with 8-core processor Intel 3.4 GHz CPUs and 16 GB of memory. In this computational environment, a total of 65 h was required to calculate 1000 steps. In order to increase the accuracy of the analysis, a steady state analysis was performed to obtain the initial values of an unsteady analysis.

3. CFD Results

3.1 Pressure Fluctuation

The pressure distribution is shown in Fig. 4. Figures 4(a) and (b) show azimuth angles of 0° and 180°, respectively, at a design velocity of 3 m/s. Figures 5 and 6 show the pressure contours at azimuth angles of 180° and 0°, respectively. The pressure between the blade and the tower changes instantly, depending on the angle of the blade. This change affects the blade and tower. This phenomenon cannot be seen using an isolated rotor analysis.

The pressure distributions of the rotor surfaces show a decrease as one of the three blades passes by the tower. Then, the pressure on the tower's surface increases when the blade gradually moves away from the tower. The blade pressures on three spanwise sections (tip, 70%, and 50% locations of the blade) are shown in Figs. 7–9, respectively. A rapid pressure decrease occurs when the blade approaches the tower. The pressure patterns of the regions have similar trends. However, the pressure drop is 3.98% at the 50% location, 3.06% at the 70% location, and 1.22% at the tip location.

3.2 Force Fluctuation

Figure 10 shows a plot of the normal force on the rotor in the streamwise direction (global Z axis). As in the pressure plots, this force plot decreases rapidly when the blade approaches the tower. Because the rotor consists of three blades, 39.2% of the decrease and increase in force occurred three times in one revolution. Large force fluctuations can act as fatigue cyclic loads and can be caused by the rotor–tower interaction on a rotor with a constant cycle.

3.3 Vorticity Induced by Rotor–Tower Interaction

Figure 11 shows the flow field surrounding the rotor and tower using an iso-surface plot of the vorticity magnitude. The unsteady vortex from the rotor is clearly visible, and we note that the vortex street is well preserved at a location approximately 10 m downstream. The tower has a visibly strong influence on the rotor vortex shedding, causing a difference in the shedding frequencies on the upper and lower parts of the tower. This results in a dislocation with two distinct types of shedding for the upper and lower parts of the tower.

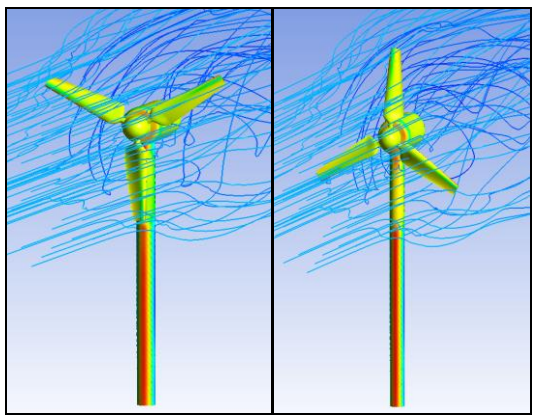

(a) (b)

Fig. 1. Pressure distributions for azimuth angles of (a) 0° and (b) 180

Table 3. Boundary condition

Description	Boundary condition
Working fluid	Water (isothermal, 25 ℃)
Rotating domain	Rotation axis (global Z) Angular velocity (TSR 5)
Inlet	Normal speed (3 m/s)
Opening	Opening
Outlet	Outlet
Interface area	GGI
Rotor and tower	Wall (no slip)
Turbulence model	SST
Total time	15 s
Time step	0.015 s
Description	Boundary condition

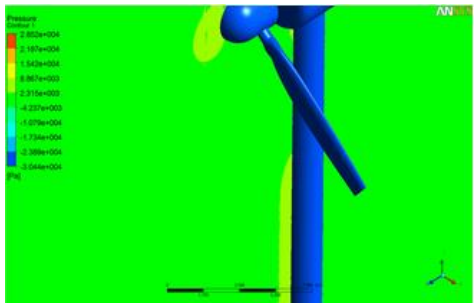

Fig. 5 Pressure contour (azimuth angle: ±180°).

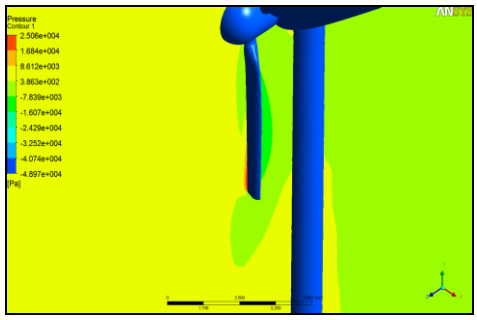

Fig. 6. Pressure contour (azimuth angle: 0°).

Fig. 7. Pressure (50% of blade radius)

Fig. 8. Pressure (70% of blade radius).

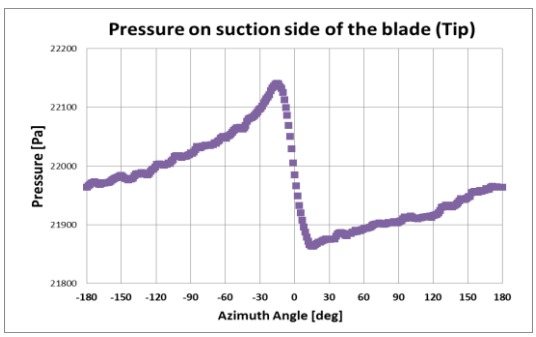

Fig. 9. Pressure (blade tip)

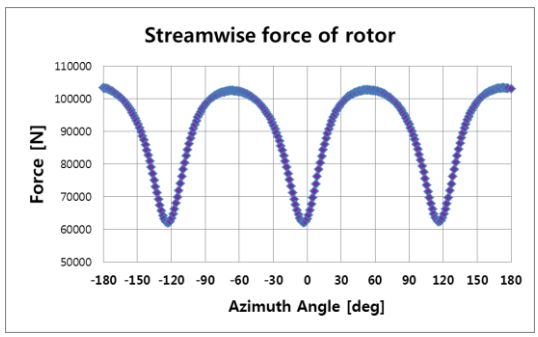

Fig. 10 Streamwise force of rotor.

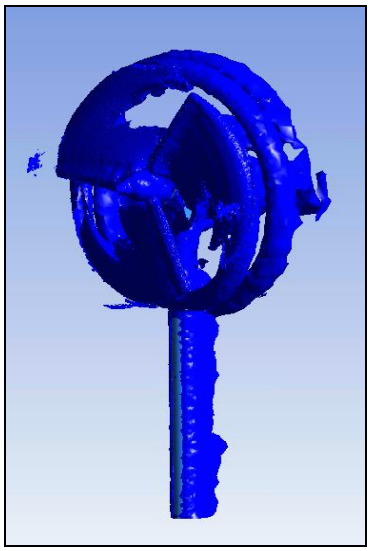

Fig. 11. Iso-vorticity plot of instantaneous flow over tower.

3. Conclusion

Our results showed that the unsteady and rotor–tower interaction played a significant role in the response of the blades. The tower exerted a significant influence on the rotor blades. Rapid changes in pressure and force occurred when the blade passed the tower. The rotor–tower interaction effect on a rotor was characterized by fluctuations in the normal force of 40% and in the pressure of 1.22 to 3.90%.

We expect that improvements can be obtained with the use of a fatigue analysis of the rotor by applying the pressure and force histories as described in this paper. In addition, it is possible that the findings of this research could be applied to vibration problems, which can affect the stability of a rotor in terms of fatigue failure or resonance.

Acknowledgements

This work is the outcome of a Manpower Development Program for Marine Energy by the Ministry of ocean and fisheries, and by Inha University. The authors are grateful to INHA University for the funding research grant.

References

[1] Chul-Hee Jo, Do-Youb Kim, Yu-Ho Rho, Kang-Hee Lee and Cameron Johnstone, “FSI analysis of deformation along offshore pile structure for tidal current power”, Renewable Energy, Vol. 54 p.248-252, 2013.

[2] Ian A. Milne, Alexander H. Day, Rajnish N. Sharma, Richard G.J. Flay and Simon Bickerton, “Tidal Turbine Blade Load Experiments for Oscillatory Motion”, 9th European Wave and Tidal Energy Conference 2011, Proceedings CD, 96th.

[3] Shigeo YOSHIDA and Soichiro KIYOKI, “Load Equivalent Tower Shadow Modeling for Downwind Turbines”, Journal of Japan Wind Energy Association, Vol. 31 p.77-85, 2007.

[4] Frederik Zahle, Niels N. Sørensen and Jeppe Johansen, “Wind Turbine Rotor-Tower Interaction Using an Incompressible Overset Grid Method”, Wind Energy, Vol.12 p.594-619, 2009.

[5] Matthias Arnold, Frank Biskup, Denis Matha and Po Wen Cheng, “Simulation of Rotor-Foundation-Interaction on Tidal Current Turbines with Computational Fluid Dynamics”, EWTEC 2013 proceedings.

[6] D. McSwiggan, T. Littler, D. J. Morrow and J. Kennedy, “Wind Turbine Rotor-Tower Interaction Using an Incompressible Overset Grid Method”, Wind Energy, Vol.12 p.594-619, 2009.